ARTICLE IN PRESS

Alexandria Engineering Journal (2020) xxx, xxx–xxx

HOSTED BY

ELSEVIER

Alexandria University

Alexandria Engineering Journal

www.elsevier.com/locate/aej
www.sciencedirect.com

Unsteady flow of Rabinowitsch fluid peristaltic transport in a non-uniform channel with temperature-dependent properties

C. Rajashekhar [a], **H. Vaidya** [b], **K.V. Prasad** [b], **Iskander Tlili** [c,d,*], **A. Patil** [e], **P. Nagathan** [e]

[a] *Department of Mathematics, Karnataka State Akkamahadevi Women's University, Vijayapur, Karnataka, India*
[b] *Department of Mathematics, Vijayanagara Sri Krishnadevaraya University, Ballari 583105, Karnataka, India*
[c] *Institute of Research and Development, Duy Tan University, Da Nang 550000, Vietnam*
[d] *Faculty of Civil Engineering, Duy Tan University, Da Nang 550000, Vietnam*
[e] *Department of Mathematics, B.L.D.E.A.'s V.P. Dr. P. G. Halakatti College of Engineering and Technology, Vijayapur, Karnataka, India*

Received 20 June 2020; revised 6 August 2020; accepted 25 August 2020

KEYWORDS

Peristaltic flow;
Rabinowitsch fluid;
Complaint walls;
Heterogeneous and homogeneous;
Variable liquid properties

Abstract Analytic results for unsteady motion of a Rabinowitsch fluid are obtained considering the variable liquid properties. The Rabinowitsch fluid is assumed to flow in an inclined non-uniform channel in the occurrence of the heterogeneous and homogeneous chemical reactions. The flow under investigation is flowing with the velocity of the wave in the wave frame of reference. The solutions of velocity, temperature, and concentration distribution are derived using the lubrication approach. Graphs are drawn for the relevant parameters to explore the characteristics of the velocity field, temperature, and streamlines. It is known that heat is nothing but the mean molecular kinetic energy, and hence the variation in velocity accounts for the corresponding difference in temperature. This behavior is noticed from the graphical representations of velocity and temperature profiles.

1. Introduction

Oscillations due to the transverse progressive waves traveling through the flexible wall result into continuous periodic oscillations of the muscular ducts called Peristalsis. The mechanism behind this is the progressive wave moving along the boundaries of the tract from the region of low pressure to high pressure through pumping action. Peristaltic flow is a well-known natural phenomenon for the mixing and transport of fluids that occur in biological tracts. It occurs in many physiological situations like transport of mixture of food grains and liquids in the esophagus, transport of urine through the ureter, in small blood vessels to transport blood, etc. This system

* Corresponding author at: Institute of Research and Development, Duy Tan University, Da Nang 550000, Vietnam.
E-mail address: iskandertlili@duytan.edu.vn (I. Tlili).

Peer review under responsibility of Faculty of Engineering, Alexandria University.

https://doi.org/10.1016/j.aej.2020.08.036
1110-0168

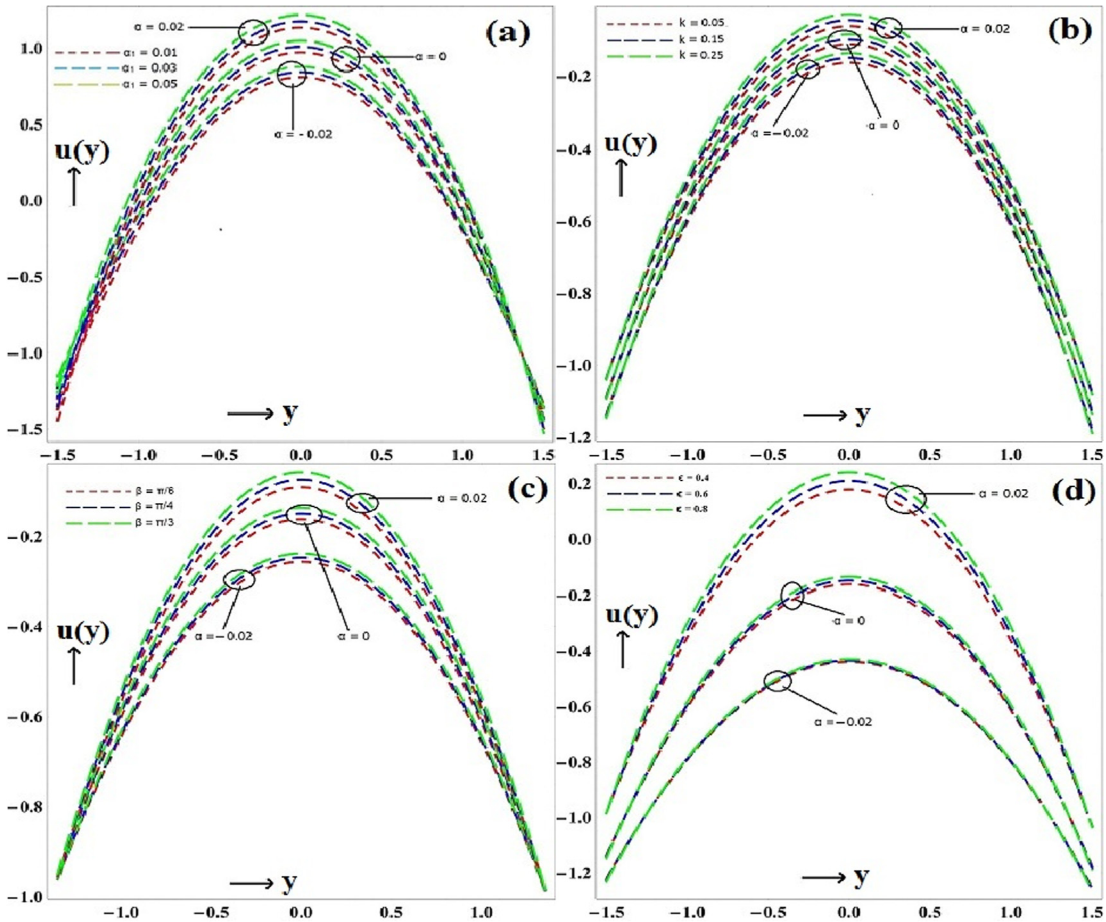

Fig. 1 Velocity plots for (a) variable viscosity α_1, (b) non-uniform parameter k, (c) angle of inclination β and (d) amplitude ratio ε.

appears in many industrial and physiological processes to pump sanitary and corrosive fluids. Currently, researchers focus on peristaltic transport due to its enormous applications ranging from a diverse field of biological systems, chemical industry, physiology, and medical procedures. The peristaltic motion under the lubrication approach has been vastly discussed by Shapiro et al. [1]. The peristaltic flow of a non-Newtonian fluid has been considered by Medhavi [2]. Presently there is a vast literature available on the subject [3–6].

In physiological problems, compliant walls are collapsing due to the fall of internal-external pressure differences less than a critical value near zero, and the muscular effect relates to the real model. Consequently, the motion follows the peristaltic mechanism. Wall tension, wall rigidity, and wall stiffness are few of the wall properties that have captured importance because of their physical significance in Peristalsis. Particularly their high intensity can considerably influence BP in humans. Elnaby and Haroun [7] deliberated the motion of a viscous fluid influenced by wall properties under Peristalsis. The peristaltic flow of Maxwell fluid through a compliant walled conduit is examined by Ali et al. [8]. Srinivas and Kothandapani [9] explored the MHD peristaltic transport to analyze the slip wall and heat flow effects. Javed et al. [10] examined the consequences of heat on a Burgers' fluid inside the peristaltic channel having compliant walls. Khan and Tariq [11] investigated the wall property influence on dusty Walter's B fluid under Peristalsis.

Reactions are being classified into heterogeneous or homogeneous depending on whether they take place as a single-phase reaction or at an interface. Various chemical reactions involve homogeneous and heterogeneous reactions, viz., destruction of crops while freezing, catalysis, cooling towers, combustion, dispersion of fog, biochemical systems, and many others. A homogeneous-heterogeneous model in boundary-layer flow is examined by Merkin [12]. Kameswaran et al. [13] explored the nanofluid flow over a shrinking/stretching sheet to analyze the effects of homogeneous-heterogeneous reactions. The sheet is positioned in a porous medium saturated with Copper-water and silver-water nanofluids, for analysis. The micropolar fluid motion over a shrinking or stretching sheet is considered to make out the effects of heterogenous-homogenous reactions numerically by Shaw et al. [14]. The flow of a magneto-Newtonian fluid through an asymmetric porous peristaltic channel is considered by Shob [15] to explore the dispersion of a solute under heterogeneous and homogeneous chemical reactions. Hayat et al. [16] examined the Carreau fluid in a peristaltic conduit with wall properties for analyzing the consequences of homogeneous-heterogeneous reactions. Hayat et al. [17] considered Peristalsis through curved geometry to investigate the homogeneous-heterogeneous reaction effects.

The last few decades have seen a lot of development in the research activities concerned with non-Newtonian fluids motion and solution to highly nonlinear equations [18–31].

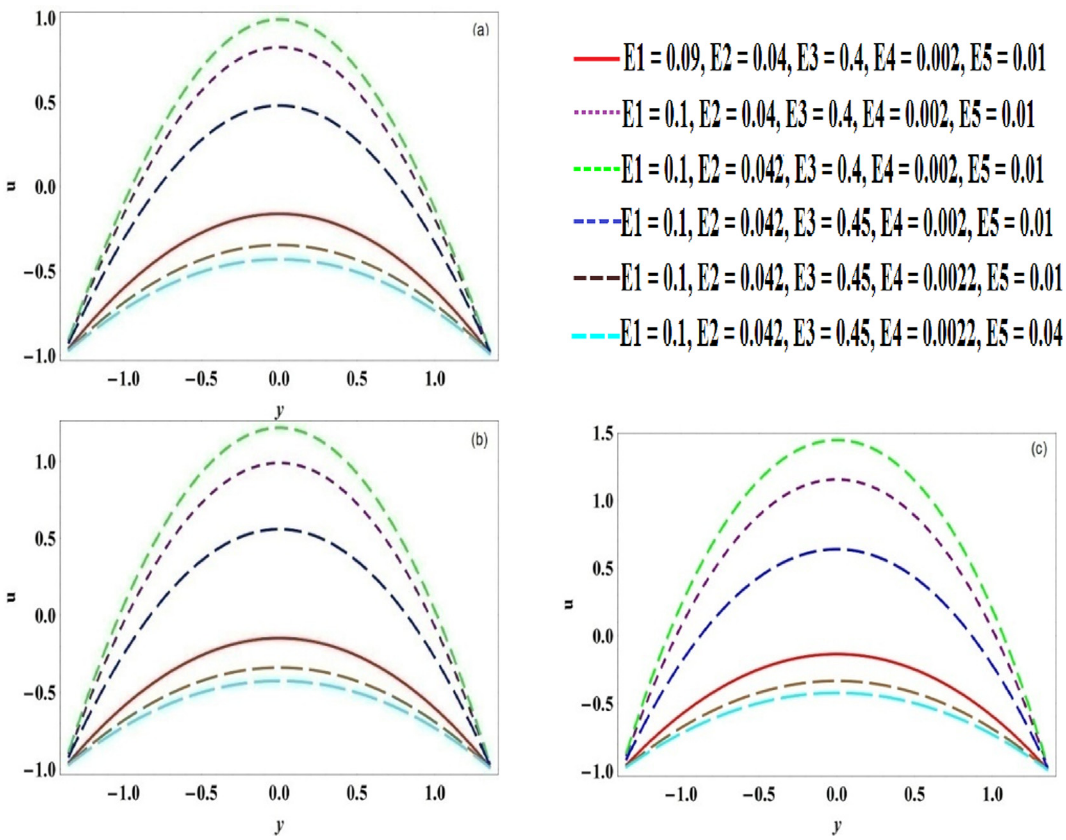

Fig. 2 Velocity Plotsfor variation in the values of wall parameters considering (a) $\alpha = -0.02$, (b) $\alpha = 0$ and (c) $\alpha = 0.02$.

The events in industry and technology and the challenges presented by the governing equations of the flow to solve mathematically can be credited for this rigorous development. The non-Newtonian fluid forms a large section of the fluids wherein the deformation rate and shear stress have a nonlinear relation. Further, no model exists that can be considered a universal constitutive model for predicting the behavior of all available non-Newtonian fluids. As a result, several constitutive models exist to illustrate their application in different fields of science and engineering. The Rabinowitsch fluid model reveals the complex rheological behaviors of biological fluids. Rabinowitsch fluid model exhibits the nonlinear association between the strain rate and shear stress. The Rabinowitsch fluid behaves differently for the nonlinear factor α, representing a Newtonian fluid for $\alpha = 0$, shear thickening fluid for $\alpha < 0$ and it represents a shear-thinning fluid for $\alpha > 0$. Akbar and Nadeem [32] explored the Rabinowitsch fluid transport under the peristaltic mechanism. Sadaf et al. [33] studied the consequences of viscous dissipation and convective boundary conditions of a Rabinowitsch fluid model in a non-uniform peristaltic tube having wall properties. Sing et al. [34] analyzed the model of Rabinowitsch fluid for homogeneous-heterogeneous reactions in an elastic peristaltic channel. Saravana et al. [35] found the consequences of heat flow on the flow of a Rabinowitsch fluid in an inclined peristaltic conduit having compliant walls. The peristaltic mechanism through an inclined porous convective channel is reported by Vaidya et al. [36] considering the variable liquid properties of a Rabinowitsch liquid. Further, Vaidya et al. [37–39] studied the same fluid with wall and variable liquid properties. Vaidya et al. [40] examined the compliant wall effects and rheological properties of Rabinowitsch fluid through a porous peristaltic inclined channel. Recently, Imran et al. [41] studied the Rabinowitsch fluid model of peristaltic flow for simultaneous effects of heterogeneous–homogeneous reactions accompanied by thermal radiation.

Peristalsis has been inspected under thermo-physical properties like variable viscosity and variable thermal conduction; however, these can't be elementary for isotropic fluids. Comparatively, they become vital as the temperature and viscosity of the fluid keep on varying, as seen in blood. Hence it becomes crucial to study thermal conductivity as well as variable viscosity. The instability in the heat and temperature produced by the inner contacts, for lubricating fluids alter the physical characteristics of the fluid and cannot be steady again. The progress in temperature accounts for growth in the incidence of transportation. Variable liquid properties promote the broader indulgence of classical and biological fluids. Nadeem et al. [42] inspected the peristaltic transport under heat transfer and variable viscosity. Khan et al. [43] examined the properties of variable viscosity in the peristaltic transport of a Jeffrey fluid in a permeable asymmetric channel. The motion of non-Newtonian fluid in an inclined peristaltic porous medium, to ascertain the consequences of variable viscosity in a conduit having slip boundary conditions, was considered by Khan et al. [44]. Lachihebi [45] examined the peristaltic flow of a Newtonian liquid to acknowledge the response of variable viscosity in an asymmetric channel. The

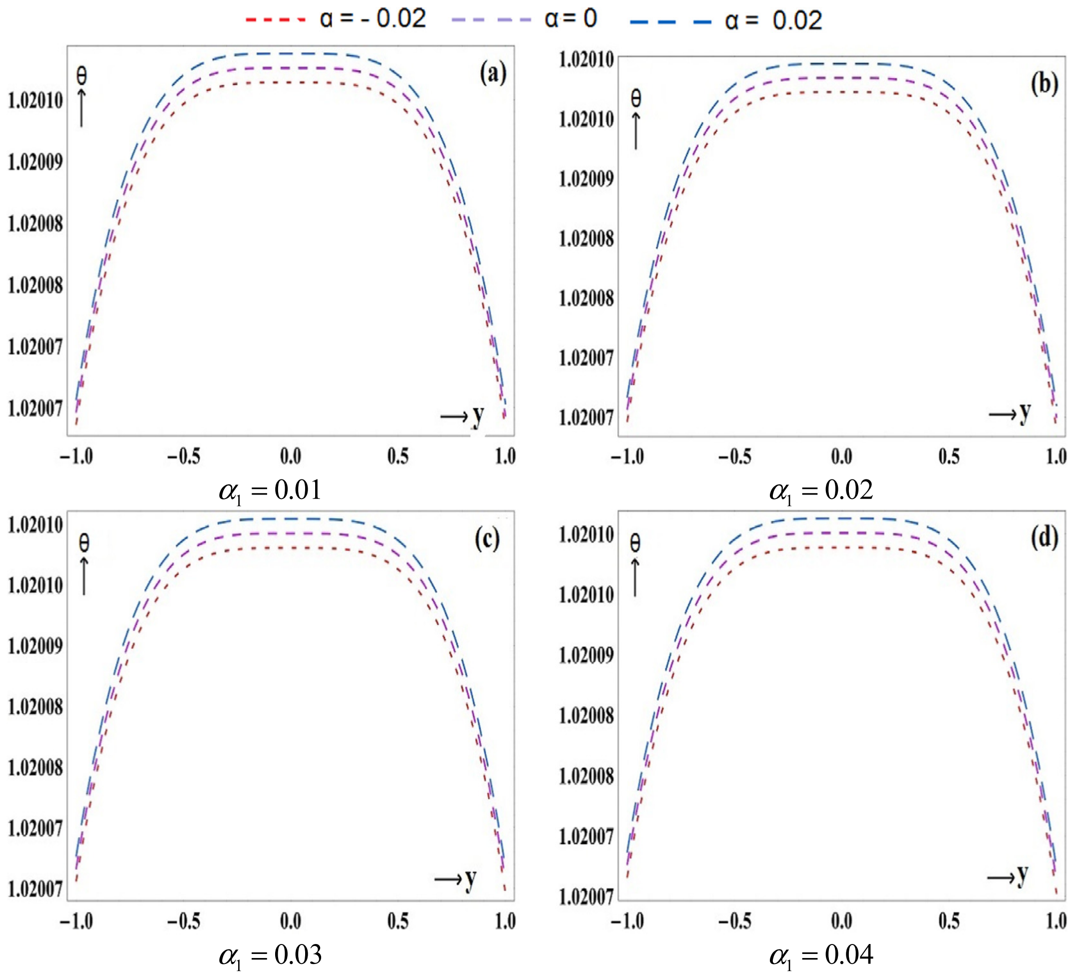

Fig. 3 Temperature plots for variation of coefficient of viscosity α_1.

flow of magneto-bio-fluid under variable thermal viscosity and heat transfer analysis inside a vertical ciliated channel is inspected by Farooq et al. [46]. Manjunath et al. [47] came out with the results of thermal conductivity and variable viscosity, heat and mass transfer on the flow of a Jeffrey fluid under the peristaltic mechanism through a non-uniform conduit with porosity. Hanumesh et al.[48] went through the MHD peristaltic transport to analyze the variable thermal conductivity and convective conditions in a complaint porous channel accompanied by heat and mass transfer.

Acknowledging the above research, it is noticed that the work on chemical reactions along with variable properties has not been carried out in the literature. Therefore, the present paper emphaizes on the impact of chemical reactions on the peristaltic flow of Rabinowitsch fluid moving through a non-uniform channel. Furhter, the variation in viscosity and thermal conductivity are taken into consideration for the flow of incompressible fluid flowing through compliant wall. Governing equations for the problem under consideration have been simplified under the lubrication approach. Solutions are evaluated for mean velocity and streamlines using the perturbation method. Physical behaviors of different parameters of Rabinowitsch fluid flow are explored graphically.

2. Mathematical formation

A flow of an incompressible Rabinowitsch fluid in a non-uniform channel between two flexible walls is modeled under peristaltic motion. The channel is symmetric and inclined to the axis. The movement of the liquid is induced by the peristaltic wave trains accelerating at a constant speed c. The deformation in the channel walls due to the peristaltic waves is represented by:

$$\bar{h}\,(\bar{X},\bar{t}) = l(\bar{X}) + b\ \mathrm{Sin}\left[\frac{2\pi}{\lambda}\left(\bar{X} - c\,\bar{t}\right)\right] \tag{1}$$

where geometry of the sinusoidal wave is represented by $\bar{h}$, non-uniform channel width by $l(\bar{X})$, wave amplitude by b and the time by t.

The chemical species A and B react under homogeneous-heterogeneous effectas describedbelow:

$$A + 2B \rightarrow 3B, \quad \text{rate} = k_c\,\bar{\varsigma}\,\bar{\xi}^{2}. \tag{2}$$

We also find the independent, first-order chemical and isothermal reactions on the surface of the catalyst. Thus, we have

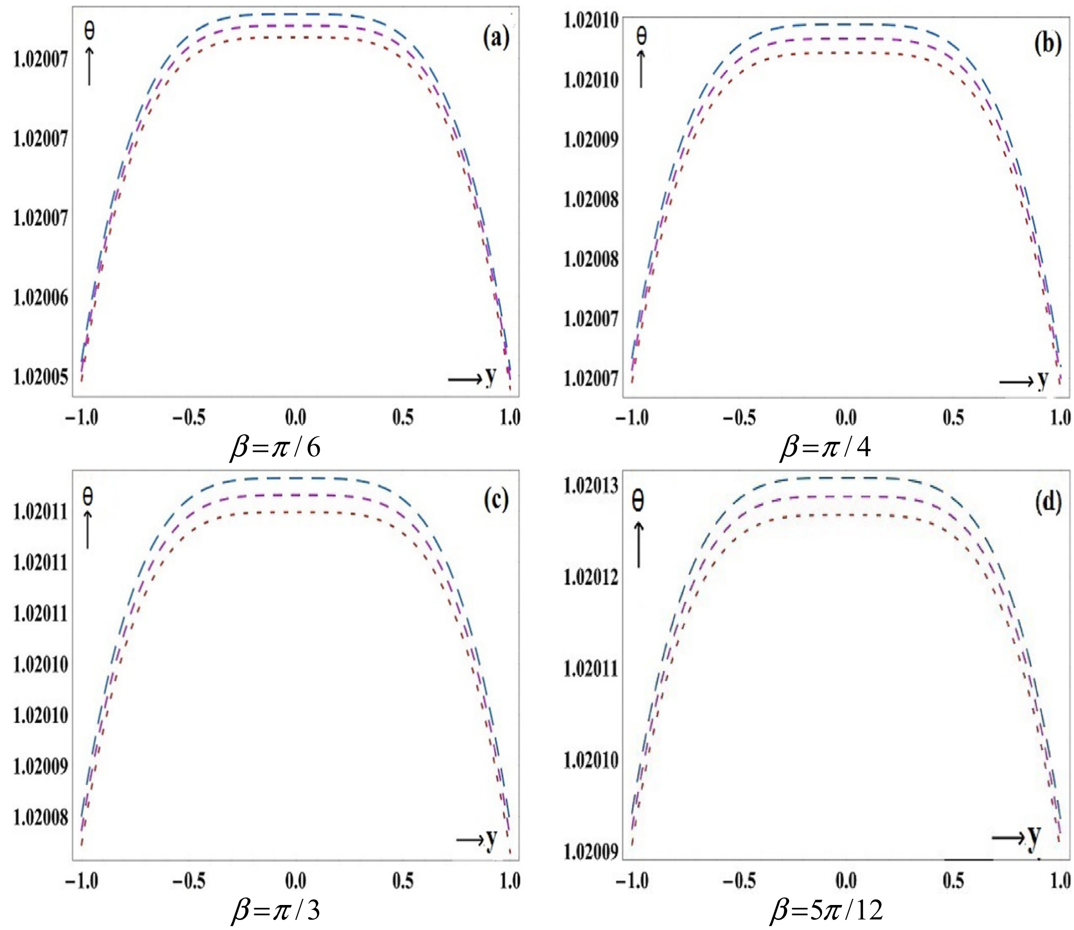

Fig. 4 Temperature plots for variation of angle of inclination β.

$$A \rightarrow B, \quad \text{rate} = k_s\,\bar{\varsigma} \tag{3}$$

where the concentration of A and B are respectively $\bar{\varsigma}$ and $\bar{\xi}$, the rate constants are k_c and k_s. It is necessary to remember that all mechanisms of such reactions exist at the same temperature.

The two-dimensional governing equations of the fluid motion in the laboratory frame is given by

$$\frac{\partial \bar{U}}{\partial \bar{X}} + \frac{\partial \bar{V}}{\partial \bar{Y}} = 0, \tag{4}$$

$$\rho\left(\frac{\partial \bar{U}}{\partial \bar{t}} + \bar{U}\frac{\partial \bar{U}}{\partial \bar{X}} + \bar{V}\frac{\partial \bar{U}}{\partial \bar{Y}}\right) = -\frac{\partial \bar{P}}{\partial \bar{X}} + \frac{\partial \bar{\tau}_{\bar{X}\bar{X}}}{\partial \bar{X}} + \frac{\partial \bar{\tau}_{\bar{X}\bar{Y}}}{\partial \bar{Y}} + \rho g\,\mathrm{Sin}\beta, \tag{5}$$

$$\rho\left(\frac{\partial \bar{V}}{\partial \bar{t}} + \bar{U}\frac{\partial \bar{V}}{\partial \bar{X}} + \bar{V}\frac{\partial \bar{V}}{\partial \bar{Y}}\right) = -\frac{\partial \bar{P}}{\partial \bar{Y}} + \frac{\partial \bar{\tau}_{\bar{X}\bar{X}}}{\partial \bar{X}} + \frac{\partial \bar{\tau}_{\bar{X}\bar{Y}}}{\partial \bar{Y}} - \rho g\,\mathrm{Cos}\beta, \tag{6}$$

$$\rho c_p\left(\frac{\partial \bar{T}}{\partial \bar{t}} + \bar{U}\frac{\partial \bar{T}}{\partial \bar{X}} + \bar{V}\frac{\partial \bar{T}}{\partial \bar{Y}}\right) = \frac{\partial}{\partial \bar{X}}\left(k(\bar{T})\frac{\partial \bar{T}}{\partial \bar{X}}\right) + \frac{\partial}{\partial \bar{Y}}\left(k(\bar{T})\frac{\partial \bar{T}}{\partial \bar{Y}}\right) + \bar{\tau}_{\bar{X}\bar{X}}\frac{\partial \bar{U}}{\partial \bar{X}} + \bar{\tau}_{\bar{Y}\bar{Y}}\frac{\partial \bar{V}}{\partial \bar{Y}} + \bar{\tau}_{\bar{X}\bar{Y}}\left(\frac{\partial \bar{V}}{\partial \bar{X}} + \frac{\partial \bar{U}}{\partial \bar{Y}}\right) = 0, \tag{7}$$

$$\frac{d\bar{\varsigma}}{d\bar{t}} = M_A\left(\frac{\partial^2 \bar{\varsigma}}{\partial \bar{X}^2} + \frac{\partial^2 \bar{\varsigma}}{\partial \bar{Y}^2}\right) - K_c\,\bar{\varsigma}\,\bar{\xi}^2, \tag{8}$$

$$\frac{d\bar{\xi}}{d\bar{t}} = M_B\left(\frac{\partial^2 \bar{\xi}}{\partial \bar{X}^2} + \frac{\partial^2 \bar{\xi}}{\partial \bar{Y}^2}\right) + K_c\,\bar{\xi}\,\bar{\varsigma}^2. \tag{9}$$

The equivalent boundary conditions are

$$\frac{d\bar{U}}{d\bar{Y}} = 0,\ \frac{d\bar{T}}{d\bar{Y}} = 0,\ \bar{\varsigma} = \varsigma_0,\ \bar{\xi} = 0 \quad \text{at} \quad \bar{Y} = 0, \tag{10}$$

$$\bar{U} = -1,\ \bar{T} = 1,\ D_A\frac{d\bar{\varsigma}}{d\bar{Y}} = k_s\,\bar{\varsigma},\ D_B\frac{d\bar{\xi}}{d\bar{Y}} = -k_s\,\bar{\xi} \quad \text{at} \quad \bar{Y} = \bar{h}. \tag{11}$$

The flexible wall motions equation is governed by

$$L(P) = P - P_0, \tag{12}$$

where $P_0(=0)$ indicates the pressure on the outer wall due to the tension of muscles. Here the linear operator L infers the membrane stretching accompanied by the focus of viscous damping and is represented as

$$L = -\tau\frac{\partial^2}{\partial x^2} + m_1\frac{\partial^2}{\partial t^2} + m_2\frac{\partial}{\partial t} + m_3\frac{\partial^4}{\partial x^4} + H, \tag{13}$$

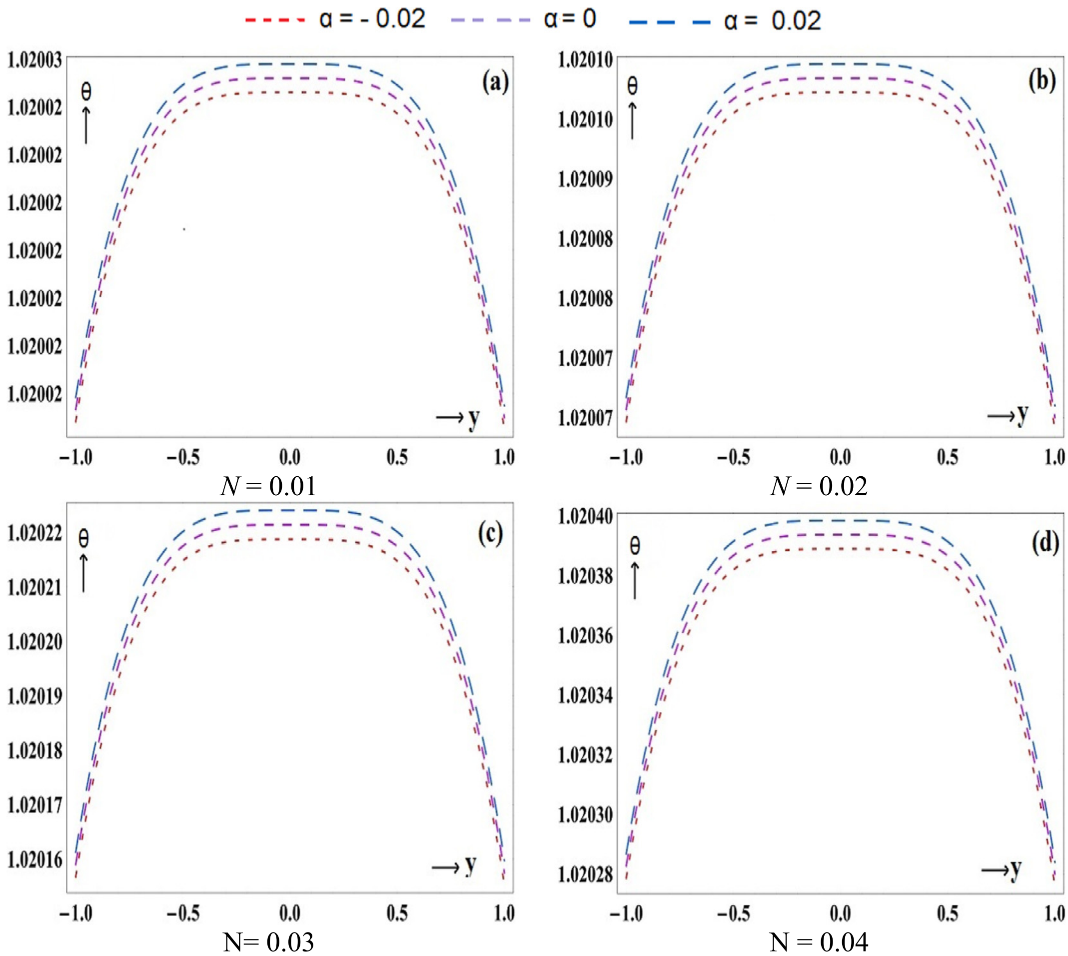

Fig. 5 Temperature plots for variation of Brinkmann number N.

where τ denotes the elastic tension, H denotes the spring stiffness, m_1 denotes the mass/unit area, m_2 denotes the coefficient of the wall damping force, m_3 denotes the flexible rigidity of the plate.

$$\frac{\partial p}{\partial x} = E_1\frac{\partial^3 h}{\partial x^3} + E_2\frac{\partial^3 h}{\partial x\partial t^2} + E_3\frac{\partial^2 h}{\partial x\partial t} + E_4\frac{\partial^5 h}{\partial x^5} + E_5\frac{\partial h}{\partial x}. \tag{14}$$

The constitutive equation of Rabinowitsch fluid in the dimensional form is:

$$\tau_{xy} + \mu_1\tau_{xy}^3 = \mu\frac{\partial u}{\partial y}, \tag{15}$$

where μ symbolizes the fluid viscosity and μ_1 the coefficient of pseudoelasticity. The unsteady flow in a stationary frame is considered to become steady in the moving frame of reference. The interrelated transformations among stationary coordinates $(\bar X, \bar Y)$ and varying coordinates $(\bar x, \bar y)$ are given by

$$\bar x = \bar X - c\,\bar t,\ \bar y = \bar Y,\ \bar u(\bar x, \bar y) = \bar U(\bar X, \bar Y, \bar t) - c,\ \bar v(\bar x, \bar y) = \bar V(\bar X, \bar Y, \bar t),\ \bar T(\bar x, \bar y) = \bar T(\bar X, \bar Y, \bar t),\ \bar p(\bar x, \bar y) = \bar P(\bar X, \bar Y, \bar t). \tag{16}$$

The following dimensionless parameters are used fornondimensionalisation:

$$x = \frac{\bar x}{\lambda},\ y = \frac{\bar y}{l_2},\ u = \frac{\bar u}{l_2},\ t = \frac{c\,\bar t}{\lambda},\ p = \frac{\bar p\, l_2^2}{\lambda\mu_0 c},\ \varepsilon = \frac{b}{l_2},\ Re = \frac{\rho c l_2}{\mu_0},$$
$$Pr = \frac{\mu_0 c_p}{k},\ Ec = \frac{c^2}{c_p\left(\bar T_1 - \bar T_0\right)}, \theta = \frac{\bar T - \bar T_0}{\bar T_1 - \bar T_0},$$
$$l(\bar x) = l_2 + m_1(\bar x),\ N = Ec\Pr,\ Sc = \frac{\gamma}{D},\ \bar\varsigma = \frac{f}{\varsigma_0},$$
$$\bar\xi = \frac{g}{\xi_0}, \gamma = \frac{M_B}{M_A}, E_1 = \frac{-\tau l_2^3}{\lambda\mu_0^3 c}, E_2 = \frac{m_1 c l_2^3}{\lambda^3\mu_0},\ E_3 = \frac{m_2 l_2^3}{\lambda^3\mu_0},$$
$$E_4 = \frac{m_3 l_2^3}{\lambda^3\mu_0 c},\ E_5 = \frac{H l_2^3}{\lambda\mu_0 c}, F = \frac{\rho c}{\mu_0 g l_2^2}, \bar\mu_0 = \frac{\mu_0}{\mu}, \bar\tau_{\bar x\bar y} = \frac{l_2\tau_{xy}}{\mu_0 c},$$
$$\bar\tau_{\bar x\bar x} = \frac{l_2\tau_{xx}}{\mu_0 c},\ \bar\tau_{\bar y\bar y} = \frac{l_2\tau_{yy}}{\mu_0 c}, h = \frac{\bar h}{l_2} = 1 + \frac{\lambda m x}{l_2}$$
$$+ \varepsilon\sin(2\pi(x - t)),\ \alpha = \frac{\mu_0^2 c^2\mu_1}{l_2^2}. \tag{17}$$

Therefore, incorporating the lubrication approach to the equations (4) – (9) and using the non-dimensionquantities in Eq. (17), the differential equations govern the current fluid flow problem:

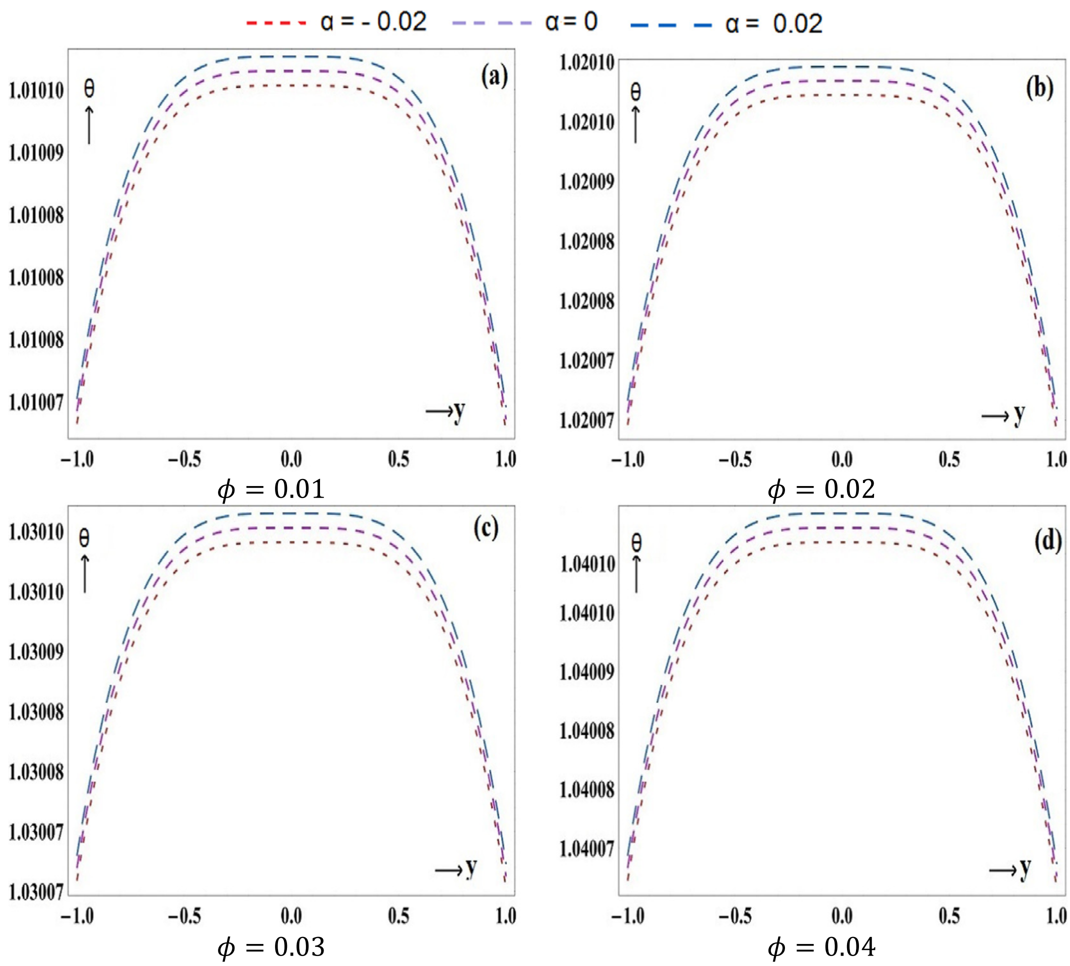

Fig. 6 Temperature plots for variation of thermal conductivity φ.

$$\frac{dp}{dx} = \frac{\partial \tau_{xy}}{\partial y} + \frac{\mathrm{Sin}\,\beta}{F}, \tag{18}$$

$$\frac{\partial p}{\partial y} = 0, \tag{19}$$

$$\frac{\partial}{\partial y}\left(k(\theta)\frac{\partial \theta}{\partial y}\right) + N\tau_{xy}\left(\frac{\partial u}{\partial y}\right) = 0, \tag{20}$$

$$\frac{1}{Sc}\frac{\partial^2 f}{\partial y^2} - Kfg^2 = 0, \tag{21}$$

$$\frac{\gamma}{Sc}\frac{\partial^2 g}{\partial y^2} + Kfg^2 = 0. \tag{22}$$

The equivalent boundary conditions after non-dimensionalisation are

$$\frac{du}{dy} = 0,\ \frac{d\theta}{dy} = 0,\ f = 0,\ g = 0 \ \text{ at } \ y = 0, \tag{23}$$

$$u = -1,\ \theta = 1,\ \frac{df}{dy} = k_s f,\ \frac{dg}{dy} = -k_s g \ \text{ at } \ y = h. \tag{24}$$

Generally, A and B, the diffusion coefficient of chemical species are not equal, but as a special case, it may be assumed that they are equivalent in size and therefore $M_A = M_B$ i.e. $\gamma = 1$. This assumption gives:

$$f + g = 1. \tag{25}$$

Hence,

$$\frac{1}{Sc}\frac{\partial^2 f}{\partial y^2} + Kf(1-f)^2 = 0. \tag{26}$$

Correspondingly conditions at the boundary are:

$$f = 1, \ \text{ at } \ y = 0 \ \text{ and } \ \frac{df}{dy} = k_s f \ \text{ at } \ y = h. \tag{27}$$

The constitutive equation of Rabinowitsch fluid in the nondimensional form is given by [35–38]

$$\tau_{xy} + \alpha\tau_{xy}^3 = \mu(y)\frac{\partial u}{\partial y} \tag{28}$$

Here α denotes the coefficient of pseudoplasticity: the non-linear factor accountable for non-Newtonian behavior of the fluid and exhibits a fundamentalpart in knowing the nature of the fluid, and μ denotes the viscosity of the fluid. The model stated above acts as a dilatant, Newtonian, and pseudoplastic fluid according as $\alpha < 0$, $\alpha = 0$ and $\alpha > 0$.

Every day, a similar-sized human or animal consumes 1–2 L of fluid. Thesmall intestine receives 6–7 L of the fluid as secretions from not only thesmall intestine itself but also the stomach, liver pancreas, salivary glands. This reflects the dependency of fluid concentration on the spatial coordinate y. Also, it is shown that blood cells are more concentrated near

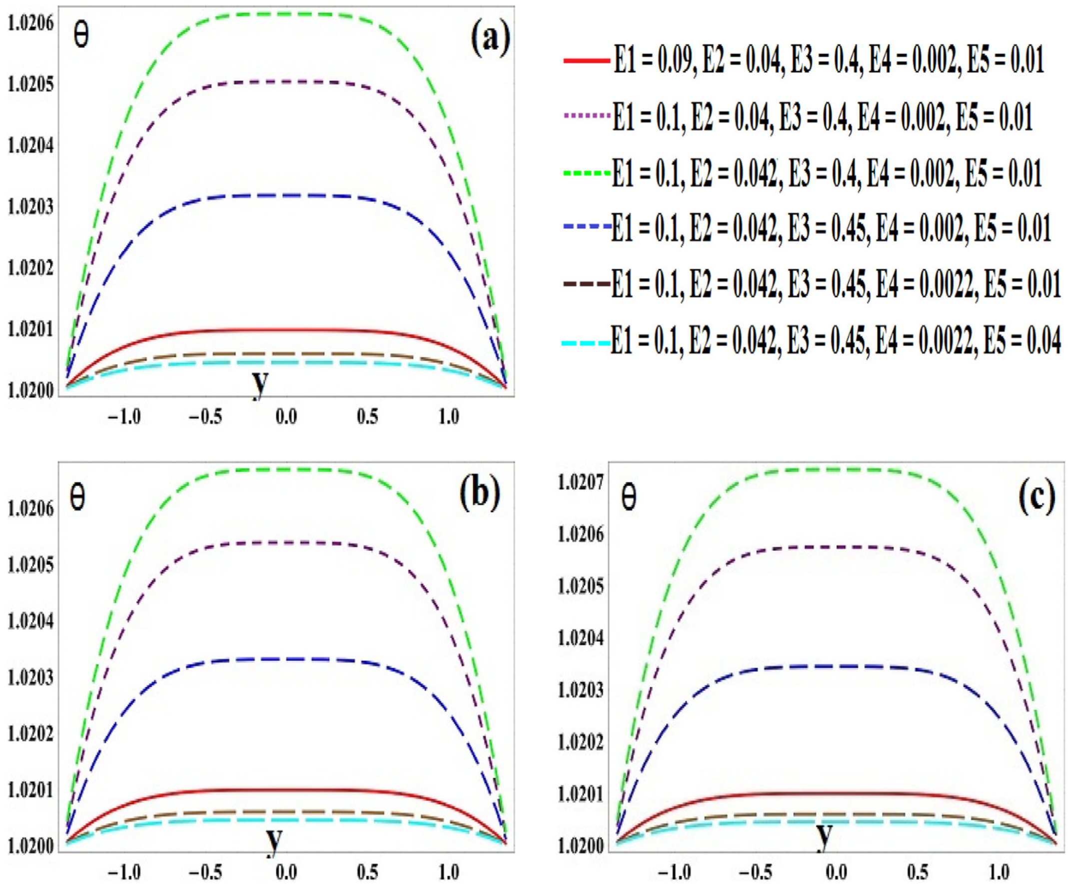

Fig. 7 Temperature plots for variation of wall parameters considering (a) $\alpha = -0.02$, (b) $\alpha = 0$ and (c) $\alpha = 0.02$.

the center of the arteries and a thin layer of clear plasma is found close to the walls. So, the viscosity of the fluid close to the walls is less than that away from it. Further, the fluid thermal conductivity varies with temperature. The expressions for variable viscosity and thermal conductivity are given by

$$\mu(y) = 1 - \alpha_1 y \quad \text{for} \quad \alpha_1 << 1 \tag{29}$$

$$k(\theta) = 1 + \varphi\theta \; for \, \varphi << 1, \tag{30}$$

where the coefficient of viscosity is α_1 andthe coefficient of thermal conductivity is φ.

3. Method of solution

To get a solution for the velocity field, Eq. (18) along with boundary conditions (23) and (24), are solved analytically and obtained as

$$u = \frac{1}{6\alpha_1^4}\left(6(P-B)^2\alpha(\log(1-h\alpha_1)) - \log(1-y\alpha_1)\right) + \alpha_1\left(6(P-B)^3(h-y)\alpha + \alpha_1\left(\begin{array}{l} 3(P-B)\left((P-B)^2(h-y)(h+y)\alpha \right. \\ \left. +2\log(1-h\alpha_1) - 2\log(1-y\alpha_1)\right) + \\ \left(3(P-B)(h-y) + (P-B)^2(h^2-y^2)\alpha - 3\alpha_1\right)\alpha_1 \end{array}\right)\right) \tag{31}$$

where $P = \frac{\partial p}{\partial x} = 8\varepsilon\pi^3\left[\frac{E_3}{2\pi}\sin 2\pi(x-t) - \left(E_1 + E_2 - 4\pi^2 E_4 - \frac{E_5}{4\pi^2}\right)\cos 2\pi(x-t)\right]$ and $B = \frac{\sin\beta}{F}$.

The temperature and homogeneous/heterogeneous equations are nonlinear and hence it is not simple to solve the problem and obtain a closed-form solution. As a result, the perturbation technique is applied to obtain a solution. We use variable thermal conductivity (φ) and homogeneous reaction parameter (K) as perturbation parameters for finding temperature and concentration profiles, respectively.

$$\theta = \theta_0 + \varphi\theta_1 + \varphi^2\theta_2 + \mathrm{O}(\varphi^3), \tag{32}$$

$$f(y) = f_0 + kf_1 + k^2 f_2 + O(k^3). \tag{33}$$

3.1. Zeroth order system

$$\frac{\partial}{\partial y}\left((1+\varphi\theta_0)\frac{\partial\theta_0}{\partial y}\right) + N\tau_{xy}\frac{\partial u}{\partial y} = 0, \tag{34}$$

$$\frac{1}{Sc}\frac{\partial^2 f_0}{\partial y^2} = 0, \tag{35}$$

$$\theta_0 = 1 \quad \text{and} \quad \frac{\partial f_0}{\partial y} = k_s f_0 \quad at \quad y = h, \tag{36}$$

$$\frac{\partial\theta_0}{\partial y} = 0 \quad \text{and} \quad f_0 = 1 \quad at \quad y = 0. \tag{37}$$

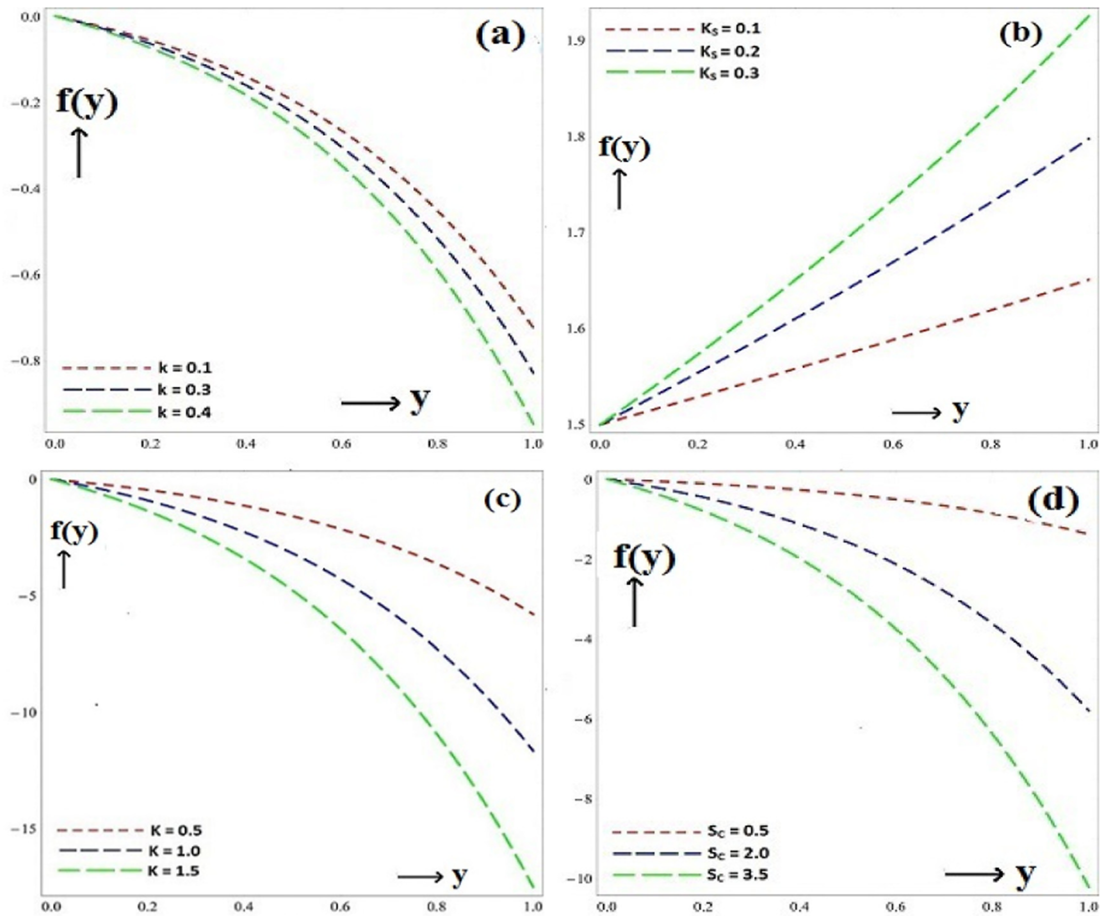

Fig. 8 Plots of Velocity $f(y)$ for variation in the values of wall parameters considering non-uniform parameter k, (b) heterogeneous reaction parameter K_s, (c) homogenous reaction parameters K, (d) Schmidt number Sc.

3.1.1. Zeroth order solution

!

$$\theta_0 = \frac{1}{60\alpha_1^6}\left[\begin{array}{c} 10\alpha_1^3\left(6\alpha_1^3 + (P-B)^2 N\begin{pmatrix} 6\,(h-y) \\ +3\alpha_1(y^2-h^2)+\alpha_1^2(y^3-h^3) \end{pmatrix}\right)+ \\ \alpha_1(P-B)^4 N\left(\begin{array}{c} -h\left(\begin{pmatrix} -60+\alpha_1 h \\ 30 \\ +\alpha_1 h(10+\alpha_1 h(5+3h)) \end{pmatrix}\right)- \\ 60y+30\alpha_1 y^2+10\alpha_1^2 y^3 \\ +5\alpha_1^3 y^4 + 3\alpha_1^4 y^5 \end{array}\right)\alpha \\ +60(P-B)^2 N\begin{pmatrix} \alpha_1^2 \\ +(P-B)^2\alpha \end{pmatrix}\begin{pmatrix} (1-\alpha_1 h)\log(1-\alpha_1 h) \\ -(1-\alpha_1 y)\log(1-\alpha_1 y) \end{pmatrix} \end{array}\right]. \tag{38}$$

$$f_0 = e^{y\,k_s}. \tag{39}$$

3.2. First-order system

$$\frac{\partial}{\partial y}\left((1+\varphi\theta_1)\frac{\partial\theta_1}{\partial y}\right) + N\tau_{xy}\frac{\partial u}{\partial y} = 0, \tag{40}$$

$$\frac{1}{Sc}\frac{\partial^2 f_1}{\partial y^2} + k_s f_0(1-f_0)^2 = 0, \tag{41}$$

$$\theta_1 = 1 \quad \text{and} \quad \frac{\partial f_1}{\partial y} = k_s f_1 \quad at \quad y = h, \tag{42}$$

$$\frac{\partial\theta_1}{\partial y} = 0 \ \text{and}\ f_1 = 1 \quad at\ \ y = 0. \tag{43}$$

3.2.1. First-order solution

$$\theta_1 = \theta_0^2, \tag{44}$$

$$f_1 = \frac{1}{6k_s^2}\begin{pmatrix} 6e^{hk_s}Sc - 6e^{2hk_s}Sc + 2e^{3hk_s}Sc + 5e^{yk_s}Sc \\ -6e^{2yk_s}Sc + e^{3yk_s}Sc - 6e^{hk_s+yk_s}Sc \\ +6e^{2hk_s+yk_s}Sc - 2e^{3hk_s+yk_s}Sc + 6e^{yk_s}Scyk_s + 6e^{yk_s}k_s^2 \end{pmatrix}. \tag{45}$$

Further, the stream function is obtained from the expression $u = \frac{\partial\psi}{\partial y}$ with the condition $\psi = 0$ at $y = 0$, which yields

$$\psi = \frac{1}{12\alpha_1^5}\left[\alpha_1\left(\begin{array}{c} 12(P-B)^3\alpha\log(1-y\alpha_1)+ \\ 12(P-B)^3 y\alpha + (1+\log(1-h\alpha_1)-\log(1-y\alpha_1)) \\ +\alpha_1\left(\begin{array}{c} 6(P-B)^3(2h-y)y\alpha + 12(P-B)\log(1-y\alpha_1)+ \\ y\alpha_1\left(\begin{array}{c} 2(P-B)\left(\begin{array}{c} 6+(P-B)^2(3h^2-y^2)\alpha + 6\log(1-h\alpha_1) \\ -6\log(1-y\alpha_1) \end{array}\right)+ \\ (P-B)\left(12h-6y+(P-B)^2(4h^3-y^3)\alpha\right)\alpha_1 - 12\alpha_1^2 \end{array}\right) \end{array}\right) \end{array}\right)\right]. \tag{46}$$

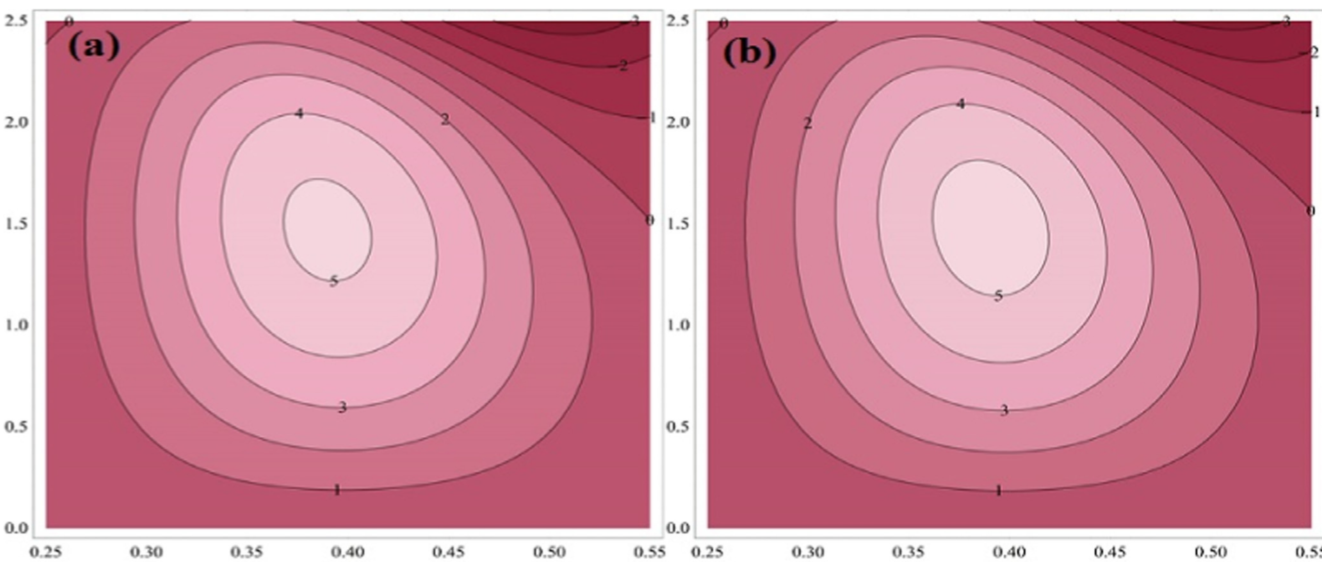

Fig. 9 Streamlines for varying non-uniformparameter:(a)$k = 0.03$ and (b)$k = 0.07$.

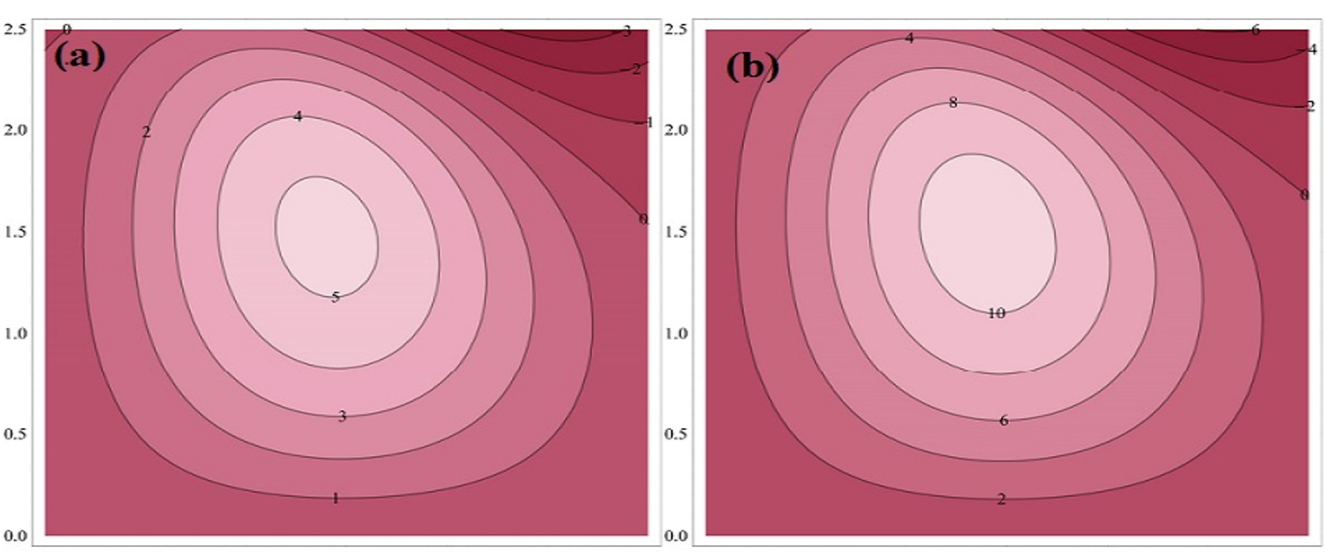

Fig. 10 Streamlines for varying variable viscosity: (a) $\alpha_1 = 0.02$ and (b) $\alpha_1 = 0.04$.

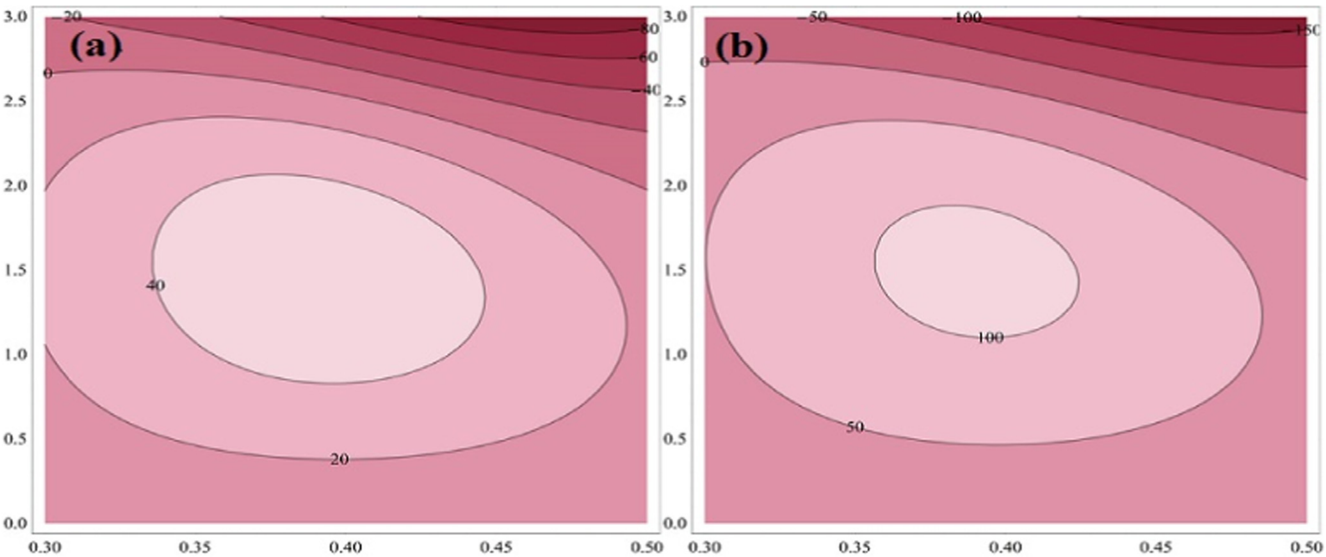

Fig. 11 Streamlines for varying pseudoplastic parameter: (a)$\alpha = 0.02$ and (b) $\alpha = 0.04$.

4. Graphical results and discussion

The results of influential parametersupon the velocity, temperature profile, concentration and stream functions are discussedthrough graphs. Particularly, the behavior of wall parameters E_1, E_2, E_3, E_4, E_5, variable viscosity α_1, Schmidt number Sc, non-uniform parameter k, angle of inclination β, variable thermal conductivity φ, homogeneous reaction parameter K and heterogeneous reaction parameter k_s are discussed. The Rabinowitsch model considered for study acts as a pseudoplastic fluid for $\alpha > 0$, Newtonian fluid for $\alpha = 0$ and dilatant fluid for $\alpha < 0$. The nature of the velocity, temperature profile and concentration profile are observed for the fixed values of coefficient of pseudoplasticity c = -0.02, $\alpha = 0$ and $\alpha = 0.02$ along with the parameters $\varepsilon = 0.6$; $k = 0.05$; $E_1 = 0.09$; $E_2 = 0.04$; $E_3 = 0.4$; $E_4 = 0.02$; $E_5 = 0.01$; $\alpha_1 = 0.02$; $N = 0.02$; $x = 0.2$; $F = 2$; $\beta = \pi/4$; $t = 0.1$; $\varphi = 0.02$.

Fig. 1(a)–(d) shows the behavior of velocity with radial coordinate y, displaying theeffects of the coefficient of variable viscosity α_1, non-uniform parameter k, angle of inclination β and amplitude ratio ε when the pseudoplasticity parameter α takes the values:-0.02, 0, 0.02. The velocity profile increases with the increasing coefficient of variable viscosity, as shown in Fig. 1(a). In other words, velocity behaves oppositely near the upper and lower walls. Usually, physiological organs are non-uniform ducts, and from Fig. 1(b), it is revealed that the

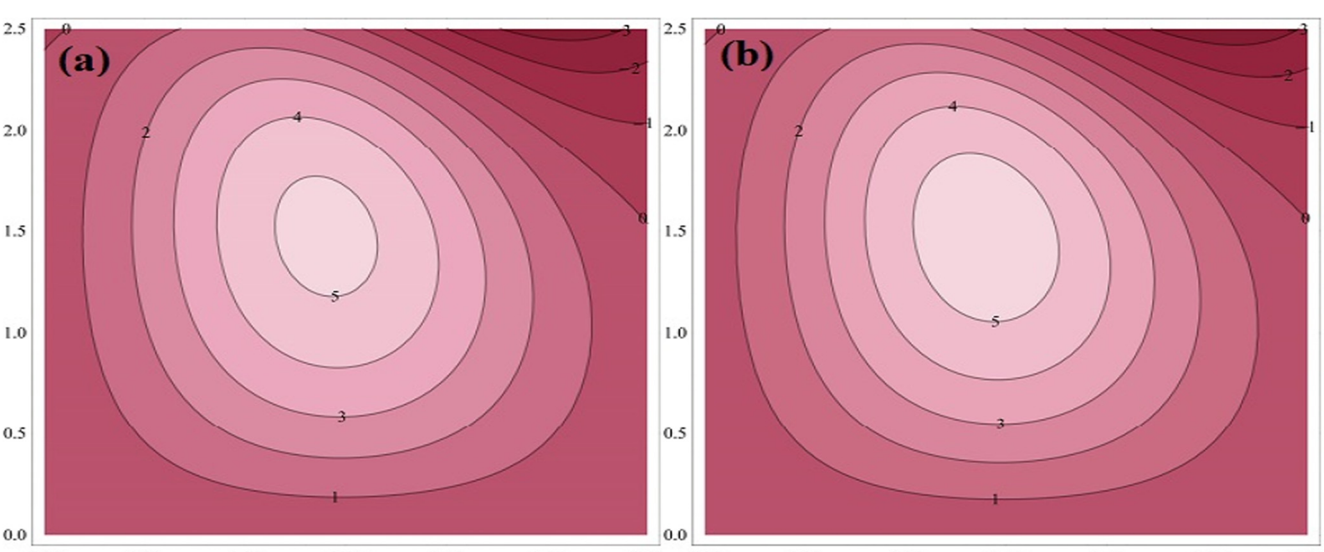

Fig. 12 Streamlines for F: (a) $F = 2$ and (b) $F = 6$.

Please cite this article in press as: C. Rajashekhar et al., Unsteady flow of Rabinowitsch fluid peristaltic transport in a non-uniform channel with temperature-dependent properties, Alexandria Eng. J. (2020), https://doi.org/10.1016/j.aej.2020.08.036

velocity profile enhances with the non-uniform parameter. Fluid velocity increase with an increase in the inclination angle due to the increased effect of gravity and is inferred from Fig. 1(c). The results of the amplitude ratio are plotted in Fig. 1(d), which exhibits a considerable increase in the velocity profile with the amplitude ratio.

The velocity profiles are plotted to study the different wall parameters E_1, E_2, E_3, E_4, E_5 (Wall tension, Mass characterization, Wall damping, Rigidity and Wall elastic parameters) as depicted in Fig. 2(a)–(c). It is observed that an enhancement in E_1 and E_2 results in increasing the values of velocity. Physically increasing values of E_1 and E_2 lessens the viscosity which develops the flow rate. Wall parameters E_3, E_4, E_5 show that velocity reduces for an increase in their values. Its reason is that for larger E_3, viscous damping improvesbecause of which velocity reduces.

Fig. 3(a)–(d) depict the temperature profile graphs for various values of the coefficient of viscosity α_1. Plots reveal that temperature gets larger with increasing variations in α_1. From Fig. 4(a)–(d) it is inferred that the temperature enhances for increasing values of inclination angle in case of dilatants, Newtonian and pseudoplastic case. It is inferred that the angle of inclination reaches maximum value nearer to the center of the channel. From Fig. 5(a)–(d) the temperature profile is increasing with growing Brinkman number N for shear thinning, thickening and viscous fluids and this result is in concurrence with Singh et al. [34]. With growing values of N, there is a stronger heat generation because the friction is utilized by shear in the motion that increases the fluid's temperature. The heat conduction capability of a material is known as thermal conductivity. From Fig. 6(a)–(d) it is accountable that increasing the thermal conductivity parameter φ escalates the temperature profile, for all the three cases. Fig. 7(a)–(c) elucidates that the temperature profile rises for all the five elastic wall parameters. It can also be noted that velocity and temperature exhibit behave similarly.

Graphs in Fig. 8(a)–(d) elucidate the behaviors of different parameters on the chemical reaction profile $f(y)$. The impact of the non-uniform parameter on the concentration profile depicts that concentration distribution reduces with non-uniformity parameters, as in Fig. 8(a). Fig. 8(b) and (c) demonstrate the contradictory nature of the strength of heterogeneous and homogenous reaction parameters. The Schmidt number is the ratio of the momentum to the mass diffusivity, shown in Fig. 8(d). The figure reveals that an increase in the Schmidt number diminishes the chemical reaction.

A cellular flow pattern is developed by the streamlines forming closed loops that flow in the channel as a trapped bolus, and the trapped bolus moves forward through the sinusoidal waves with the same speed as that of the wave. This phenomenon physically can be seen in blood movement as thrombus and blood bolus. In Fig. 9–12 contour map plots illustrate the effects of a non-uniform parameter, variable viscosity, coefficient of the pseudoplastic parameter, and body forces on trapped bolus. Trapping is analyzed for the non-uniform parameter from Fig. 9. It discloses that the bolus enlarges with a rise in the non-uniform parameter. Enhancing the variable viscosity and coefficient of pseudoplastic parameters, increase the magnitude of the trapped bolus, as shown in Figs. 10 and 11. The effect of the body force on trapping is shown in Fig. 12. The bolus develops in size as the body force increases.

5. Conclusion

In the present study, we have discussed the effects of slip, chemical reactions, and variable fluid properties on the peristaltic flow off Rabinowitsch fluid. The nonuniform inclined geometry is considered along with wall properties. Analytical solutions for velocity, temperature, concentration, and stream function are obtained and analyzed through graphs. The findings of the current model help in analyzing the flow of biological fluids under the peristaltic action. The significant findings from the present model are:

- The velocity profile increases for increasing values of coefficient of variable viscosity, non-uniform parameter, inclination angle and amplitude ratio.
- For an increase in the elastic wall parameters the velocity profileincreases.
- The temperature profile is increasingcoefficient of variable viscosity, inclination angle, Brinkman number and variable thermal conductivity.
- Increasing the elastic wall parameters increases the temperature profile.
- The concentration profile enhances with the introduction ofnon-uniform parameter, Schimidt number, heterogeneous and homogeneous chemical reactions.
- The volume of the trapped bolus enhances with variable viscosity, non-uniform parameter, coefficient ofpseudoelasticity and body force, on fluid velocity.

Declaration of Competing Interest

The authors declare that they have no known competing financial interests or personal relationships that could have appeared to influence the work reported in this paper.

Acknowledgements

The authors appreciate the constructive comments of the reviewers which led to the definite improvement in the paper.

References

[1] A.H. Shapiro, M.Y. Jaffrin, S.L. Weinberg, Peristaltic pumping with long wavelengths and low Reynolds number, J. Fluid Mech. 37 (1969) 799–825.
[2] A. Medhavi, Peristaltic pumping of a non-Newtonian fluid, Appl. Appl. Math. 3 (2008) 137–148.
[3] G. Manjunatha, C. Rajashekhar, H. Vaidya, K.V. Prasad, Peristaltic mechanism of bingham liquid in a convectively heated porous tube in the presence of variable liquid properties, Special Top. Rev. PorousMedia-An Int. J. 10 (2019) 187–201.
[4] C. Rajashekhar, G. Manjunatha, H. Vaidya, K.V. Prasad, S.U. Khan, Sami Ullah Khan, Influence of porous wall and variable liquid properties on peristaltic transport of a Bingham fluid through elastic tube, Heat Transfer Asian Research (2020).
[5] B.B. Divya, G. Manjunatha, C. Rajashekhar, H. Vaidya, K.V. Prasad, The hemodynamics of variable liquid properties on the MHD peristaltic mechanism of jeffrey fluid with heat and mass transfer, Alexandria Eng. J. 59 (2020) 693–706.
[6] G. Manjunatha, C. Rajashekhar, H. Vaidya, K.V. Prasad, O.D. Makinde, J.U. Viharika, Impact of variable transport properties

and slip effects on MHD Jeffrey fluid flow through channel, Arabian J. Sci. Eng. 45 (2020) 417–428.
[7] M.A. Elnaby, M.H. Haroun, A new model for study the effect of wall properties on peristaltic transport of a viscous fluid, Commun. Nonlinear Sci. Numer. Simul. 13 (2008) 752–762.
[8] N. Ali, T. Hayat, S. Asghar, Peristaltic flow of a Maxwell fluid in a channel with compliant walls, Chaos, Solitons Fractals 39 (2009) 407–416.
[9] S. Srinivas, M. Kothandapani, The influence of heat and mass transfer on MHD peristaltic flow through a porous space with compliant walls, Appl. Math. Comput 213 (2009) 197–208.
[10] M. Javed, T. Hayat, A. Alsaedi, Peristaltic flow of Burgers' fluid with compliant walls and heat transfer, Appl. Math. Comput 244 (2014) 654–671.
[11] A.A. Khan, H. Tariq, Influence of wall properties on the peristaltic flow of dusty Walter's B fluid, J. Braz. Soc. Mech. Sci. Eng. 40:368.28 (2018).
[12] J.H. Merkin, A model for isothermal homogeneous-heterogeneous reactions in boundary-layerflow, Math Comput Model 24 (1996) 125–136.
[13] P.K. Kameswaran, S. Shaw, P. Sibanda, P.V.S.N. Murthy, Homogeneous–heterogeneous reactions in a nano fluid flow due to a porous stretching sheet, Int J Heat Mass Transfer 57 (2013) 465–472.
[14] S. Shaw, P.K. Kameswaran, P. Sibanda, Homogeneous-heterogeneous reactions in micropolar fluid flow from a permeable stretching or shrinking sheet in a porous medium, Boundary Value Probl. 77–86 (2013) 2013.
[15] A.M. Sobh, Effects of homogeneous and heterogeneous reactions on the dispersion of a solute in MHD Newtonian fluid in an asymmetric channel with peristalsis, Brit. J. Math. Comput. Sci. 3 (2013) 664–679.
[16] T. Hayat, A. Tanveer, H. Yasmin, A. Alsaedi, Homogeneous-heterogeneous reactions in peristaltic flow with convective conditions, PLoS ONE 9 (12) (2014), https://doi.org/10.1371/journal.pone.0113851 e113851.
[17] T. Hayat, A. Tanveer, F. Alsaadi, N.D. Alotaibi, Homogeneous-heterogeneous reaction effects in peristalsis through curved geometry, AIP Adv. 5 (2015) 067172.
[18] W.L. Wilkinson, Non-Newtonian fluids. Fluid Mechanics, Mixing and Heat Transfer, Pergamon Press, London, 1960.
[19] A.H.P. Skelland, Non-Newtonian flow and heat transfer, John Wiley and Sons Inc, New York, 1967.
[20] C. Cattani, A. Paoluzzi, Boundary integration over linear polyhedra, Computer Aided Design 22 (2) (1990) 130–135.
[21] C. Cattani, Y.Y. Rushchitskii, Cubically nonlinear elastic waves: wave equations and methods of analysis, Int. Appl. Mech. 39 (10) (2003) 1115–1145.
[22] C. Cattani, Harmonic wavelet solutions of the Schrödinger equation, Int. J. Fluid Mech. Res. 30 (5) (2003) 463–472.
[23] C. Cattani, HaarWavelet-based technique for sharp jumps classification, Math. Comput. Modell. 39 (2–3) (2004) 255–278.
[24] Y. Xiao-Jun, G. Feng, A new technology for solving diffusion and heat equations, Therm. Sci. 21 (2017) 133–140.
[25] A. Cordero, J.P. Jaiswal, J.R. Torregrosa, Stability analysis of fourth-order iterative method for finding multiple roots of non-linear equations, Appl. Math. Nonlin. Sci. 4 (1) (2019) 43–56.
[26] H.M. Baskonus, H. Bulut, T.A. Sulaiman, New complex hyperbolic structures to the Lonngren-wave equation by using Sine-Gordon expansion method, Appl. Math. Nonlin. Sci. 4 (1) (2019) 141–150.
[27] E.I. Eskitascroglu, M.B. Aktas, H.M. Baskonus, New complex and hyperbolic forms for Ablowitz–Kaup– Newell-Segur wave equation with fourth order, Appl. Math. Nonlin. Sci. 4 (1) (2019) 105–112.
[28] L. Minati, L.V. Gambuzza, W.J. Thio, J.C. Sprott, M. Frasca, A chaotic circuit based on a physical memristor, Chaos, Solitons Fractals 138 (109929) (2020) 1–6.
[29] E. İlhan, İ.O. Kıymaz, A generalization of truncated M-fractional derivative and applications to fractional differential equations, Appl. Math. Nonlin. Sci. 5 (1) (2020) 171–188.
[30] J. Singh, D. Kumar, Z. Hummoich, A. Atangana, A fractional epidemiological model for computer viruses pertaining to a new fractional derivative, Applied Mathematics and Computation, 316: (2018), 504–515, Mathematics 8 (3) (2020) 341.
[31] J.L.G. Guirao, H.M. Baskonus, A. Kumar, Regarding new wave patterns of the newly extended nonlinear (2 + 1)-dimensional Boussinesq equation with fourth order, Mathematics 8 (3) (2020) 341.
[32] N.S. Akbar, S. Nadeem, Application of Rabinowitsch fluid model in peristalsis, ZeitschriftfürNaturforschungA 69 (2014) 473–480.
[33] H. Sadaf, S. Nadeem, Analysis of combined convective and viscous dissipation effects for peristaltic flow Rabinowitsch fluid model, J. Bionic Eng 14 (2017) 182–190.
[34] U.P. Singh, A. Medhavi, R.S. Gupta, S.S. Bhatti, Analysis of peristaltic transport of non-Newtonian fluids through non uniform tubes: rabinowitsch fluid model, ZeitschriftfürNaturforschung A 72 (2017) 601–608.
[35] R. Saravana, K. Vajravelu, S. Sreenadh, Influence of compliant walls and heat transfer on the peristaltic transport of a rabinowitsch fluid in an inclined channel, Z. Naturforsch. A 73 (2018) 833–843.
[36] H. Vaidya, R. Choudhari, G. Manjunatha, K.V. Prasad, Effect of variable liquid properties on peristaltic flow of a Rabinowitsch fluid in an inclined convective porous channel, Eur. Phys. J. Plus 134 (5) (2019) 231.
[37] H. Vaidya, R. Choudhari, G. Manjunatha, K.V. Prasad, Peristaltic mechanism of a Rabinowitsch fluid in an inclined channel with complaint wall and variable liquid properties, J. Braz. Soc. Mech. Sci. Eng. 41 (2019) 52.
[38] H. Vaidya, R. Choudhari, G. Manjunatha, K.V. Prasad, Effect of variable liquid properties on peristaltic transport of Rabinowitsch liquid in a convectively heated complaint porous channel, J. Central South Univ. 26 (2019) 1116–1132.
[39] H. Vaidya, R. Choudhari, G. Manjunatha, K.V. Prasad, O.D. Makinde, S. Sreenadh, Peristaltic motion of non-newtonian fluid with variable liquid properties in a convectively heated non-uniform tube: rabinowitsch fluid model, J. Enhanced Heat Transf. 26 (2019) 277–294.
[40] H. Vaidya, R. Choudhari, G. Manjunath, K.V. Prasad, Rheological properties and peristaltic of Rabinowitsch fluid through compliant porous wall in an inclined channel, J. Nanofluids 8 (2019) 970–979.
[41] N. Imran, M. Javed, M. Sohil, I. Tlilli, Simultaneous effects of heterogeneous–homogeneous reactions in peristaltic flow comprising thermal radiation: rabinowitsch fluid model, J. Mater. Res. Technol. 9 (2020) 3520–3529.
[42] S. Nadeem, T. Hayat, N.S. Akbar, M.Y. Malik, On the influence of heat transfer in peristalsis with variable viscosity, Int. J. Heat Mass Transf. 52 (2009) 4722–4730.
[43] A.A. Khan, R. Ellahi, K. Vafai, Peristaltic transport of a Jeffrey fluid with variable viscosity through a porous medium in an asymmetric channel, Recent Adv. Anal. Methods Math. Phys. (2012).
[44] A.A. Khan, R. Ellahi, M. Usman, The effects of variable viscosity on the peristaltic flow of non-Newtonian fluid through a porous medium in an inclined channel with slip boundary conditions, J. Porous Media 16–59 (2013).
[45] M. Lachiheb, On the effect of variable viscosity on the peristaltic transport of a Newtonian fluid in an asymmetric channel, Can. J. Phys 94 (2016) 1–8.
[46] A.A. Farooq, Z. Shah, E.O. Alzahrani, Heat transfer analysis of a magneto-bio-fluid transport with variable thermal viscosity through a vertical ciliated channel, Symmetry 11 (2019) 1240.

Please cite this article in press as: C. Rajashekhar et al., Unsteady flow of Rabinowitsch fluid peristaltic transport in a non-uniform channel with temperature-dependent properties, Alexandria Eng. J. (2020), https://doi.org/10.1016/j.aej.2020.08.036

[47] G. Manjunath, C. Rajashekhar, H. Vaidya, K.V. Prasad, K. Vajravelu, Impact of heat and mass transfer on the peristaltic mechanism of Jeffrey fluid in a non-uniform porous channel with variable viscosity and thermal conductivity, J. Therm. Anal. Calorim. 139 (2) (2020) 1213–1228.

[48] H. Vaidya, R. Choudhari, M. Gudekote, K.V. Prasad, O.D. Makinde, K. Vajravelu, Heat and mass transfer analysis on MHD peristaltic flow through a complaint porous channel with variable thermal conductivity and convective conditions, Physica Scripta 95 (4) (2020).

Please cite this article in press as: C. Rajashekhar et al., Unsteady flow of Rabinowitsch fluid peristaltic transport in a non-uniform channel with temperature-dependent properties, Alexandria Eng. J. (2020), https://doi.org/10.1016/j.aej.2020.08.036